

Environmental Spectroscopy and Biogeochemistry Facility

The Environmental Spectroscopy and Biogeochemistry (ES&B) Facility supports experimental and modeling studies of chemical phenomena and mechanisms on mineral and microbe surfaces and on complex heterogeneous environmental materials from soils, sediments, and groundwater zones. ES&B Facility staff members, along with other Pacific Northwest National Laboratory staff, form a multidisciplinary research team with expertise in chemistry, mineral physics, geochemistry, soil chemistry, microbiology, and hydrology and advanced computational methods.

Capabilities

Capabilities are available for materials characterization, aqueous- and solid-phase speciation and reaction/kinetic measurements, analytical environmental chemistry, molecular and thermodynamic geochemical process modeling, and intermediate-scale, reactive-transport studies.

Research includes studies on:

- surface chemistry of Fe, Mn, and Al oxides; carbonates; and layer silicates
- redox reactions of organic and metal contaminants with Fe- and Mn-containing mineral solids
- biogeochemistry of Fe(III) and Mn(IV) oxide reduction by bacteria and associated bio-mineralization processes
- mineral surface structure and dynamics by modeling and microscopy
- sorbate surface structure and dynamics on mineral surfaces by spectroscopy
- reactivity and thermodynamics of contaminants at high ionic strengths
- intermediate scale subsurface flow and transport
- molecular, thermodynamic and kinetic modeling.

The ES&B Facility consists of seven laboratories that are proximally located to facilitate multi-technique studies. For example, environmental chambers are available with spectroscopic access to allow

Instrumentation & Capabilities

- Analytical chemistry instrumentation
- Scanning probe microscopy
- Spectrophotometers
- Laser fluorescence microscopy
- Laser spectroscopy and kinetic systems
- Scanning and transmission electronic microscopies
- Mössbauer spectroscopy
- Electron paramagnetic resonance spectroscopy
- Controlled atmosphere chambers
- Computational geochemical molecular modeling software and hardware
- Hydro- and biogeochemical modeling and software
- Subsurface flow and transport experimental laboratory
- Thermodynamics measurements of aqueous and adsorption reactions

controlled-atmosphere experiments. These laboratories are located near other instruments that are integral to environmental molecular science, including high-resolution scanning and transmission electron microscopies and a variety of ultrahigh vacuum microprobe techniques for surface analyses. The seven ES&B Facility laboratories are described below.

Optical Spectroscopy Laboratory. Laser-based-fluorescence, breakdown, nonlinear, and Raman spectroscopies and microscopies are available to use in investigations of aqueous and interfacial reactions. Kinetic studies ranging from stopped-flow to ultra-fast optical pump-probe methods can be performed. Cryogenic capabilities and time-resolved detection methods from pico-second to millisecond for enhanced spectroscopic studies of solution and heterogeneous materials are available. State-of-science Fourier transform infrared (FTIR) spectrometers enable the study of various mineral-chemistry topics as well as sorbate binding mechanisms at mineral, biotic, and organic interfaces. The modular design of the spectrometers in this laboratory enables rapid changing of detector and beam-splitter combinations so researchers can readily change from the visible to the near-, mid-, or far-infrared wavelength ranges. A vacuum bench equipped with a helium-cooled bolometer and step-scanning capabilities is optimized for far-infrared measurements as well as time-resolved spectroscopy. A nitrogen-purged system equipped with a microscope and temperature-controlled mapping stage (-200 to 600°C) allows spatially resolved infrared measurements at the 60- μm level. A variety of cells are available for analyzing gas, liquid, solid, and slurry samples using a variety of techniques. Raman vibrational analyses can be obtained using the FT-Raman module and Raman microscope.

Mössbauer Spectroscopy Laboratory. Mössbauer spectrometers with cryogenic capabilities allow studies of Fe structure and redox chemistry in oxides, clays, and biogeochemical systems. Software incorporating Voigt-line fitting and quadrupole-splitting distributions enable state-of-science spectral deconvolution and fitting.

Electron Paramagnetic Resonance (EPR) Spectroscopy Laboratory. A continuous-wave, multi-frequency (S, X, and Q bands) EPR spectrometer equipped with helium-cooled cryostats and a stop-flow/freeze-quench system allows studies of free-radical reactions and electronic environments of paramagnetic species in solids, suspensions, and at surfaces.

Imaging Microscopy Laboratory. Optical and scanning-probe microscopies are available for particle imaging from millimeter to nanometer scales. An inverted optical microscope is available for time-resolved fluorescence imaging in a broad temperature range. Expertise is also available in the characterization of processes of microbial reduction and biogenic mineral formation by high-resolution transmission electron microscopy, involving lattice imaging, selected area diffraction, and energy dispersive spectrometer analysis. A state-of-science scanning-probe microscopy facility has been developed for imaging water-wet samples and microbe-water and mineral-microbe interfaces, and for characterizing a wide variety of environmental materials. A bio-atomic force microscope (AFM) scanning probe is available for protein imaging and force measurements. This new instrument will help researchers meet the special requirements of life sciences microscopy (e.g., studies of delicate biological samples under physiological conditions) and provide detailed observations of molecular structures with unprecedented resolution and without the need for rigorous

sample preparation and labeling. The system can be used for studying cellular membrane structures, drug-receptor and virus-cell binding, as well as single-molecule recognition of molecular complexes (e.g., antibody-antigen, ligand-receptor, DNA-protein, DNA-DNA, and protein-protein interactions).

Environmental Analytical Chemistry Laboratory. A wide variety of instrumentation is available for quantification of inorganic and organic contaminants and their reaction, transformation, or degradation products. State-of-science separation instruments, including gas and high-performance liquid chromatographs coupled with mass spectrometry, are available to users engaged in diverse research activities. An inductively coupled plasma mass spectrometer with laser ablation for solids analysis and a collision cell for improved detection of oxide-interfering elements (e.g., Fe) is available for broad-spectrum, high-sensitivity inorganic analyses.

Computational Geochemistry. Multiple workstations linked to the computational infrastructure of the EMSL are available for molecular-level simulations and modeling to support research in the ES&B Facility. Experts are available to perform first-principles molecular dynamics calculations of molecular liquids and solid state systems as well as electronic structure calculations either as stand-alone activity or in support of experimental or spectroscopic measurements. Thermodynamic and kinetic geochemical codes also are available to users, as are multidimensional geochemical reaction/transport codes for numerical experiments or simulations of the intermediate-scale flow and transport experiments described below.

Subsurface Flow and Transport Experimental Laboratory (SFTEL). This laboratory is uniquely equipped for intermediate-scale (i.e., meter-scale) experimentation in single-fluid and multifluid (air-water, air-nonaqueous-phase liquid [NAPL]-water, NAPL-water) porous media systems. These distinctive experimental systems allow testing of basic theories of flow and transport; studies of coupled processes involved with microbial, reactive chemical, or colloid transport; and experimental simulation of subsurface remediation scenarios. Close linkages exist between this center and the modeling facility, as both pre- and post-experiment modeling efforts are key to experimental design and interpretation. The main focus of the SFTEL is on intermediate-scale experimentation. The laboratory offers several meter-scale flow cells and columns for research in saturated and unsaturated porous media. Some of the flow cells and columns can be used in conjunction with a dual-energy gamma radiation system. The SFTEL also offers a fully automated saturation-pressure apparatus, as well as an automated system to measure fundamental hydraulic properties of soil.

Upgrades

An Asylum Research MFP-Three Dimensional AFM, situated atop a Nikon 300TE inverted optical microscope, was purchased and installed. This scanning probe microscope will be used for protein imaging and force measurements (Figure 1). This new instrument will help researchers to meet the special requirements of life sciences microscopy (e.g., studies of delicate biological samples under physiological conditions) and provide detailed observations of molecular structures with unprecedented resolution and without the need for rigorous sample preparation and labeling. The system can be used for studying cellular membrane structures, drug-receptor and virus-cell binding, as well as single-molecule recognition of molecular complexes (e.g., antibody-antigen, ligand-receptor, DNA-protein, DNA-DNA, and protein-protein interactions).

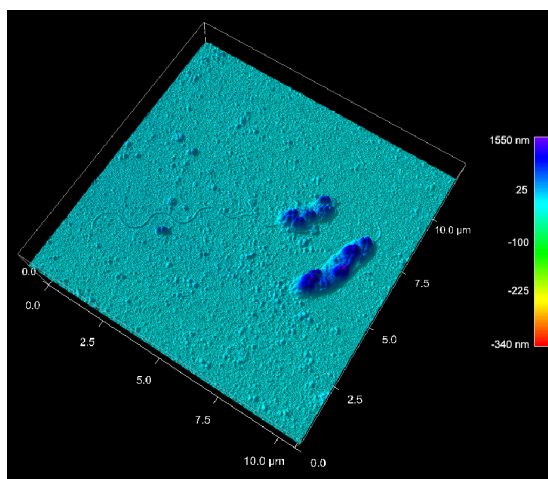


Figure 1. Three-dimensional image of *Shewanella* bacteria on hematite imaged with atomic force microscopy.

A small (50-cm) chlorinated solvent resistant flow cell was designed and constructed for use in SFTEL within EMSL's ES&B Facility. Many of the experiments conducted in this laboratory do not require the use of the larger intermediate scale flow cells (1 m). Thus, this smaller cell will allow multiple experiments to be conducted in the time it would take to pack a single large flow cell. It will also offer increased flexibility to run intermediate-scale experiments under multiple conditions more efficiently and allow testing to determine experimental parameters prior to scaling up larger flow cells. After testing of the new flow cell is complete, facility researchers will examine the effect of modifying fluids with polymer to overcome flow bypassing resulting from heterogeneity.

An ultraviolet-charge coupled diode camera and spectrograph were purchased to extend EMSL's time-resolved, laser-induced fluorescence spectroscopy and imaging spectromicroscopy capabilities into the ultraviolet region. The camera will also be used to develop laser-induced breakdown spectroscopy/detection capabilities for the investigation, detection, and quantitative analysis of environmentally important toxic metals, such as chromium, lead, arsenic, and sulfur as well as the detection of actinide-bearing aerosols and solid particles and nanocolloids *in situ*.

The Digital Instruments Bioscope AFM was upgraded. The older Nanoscope-IIIa controller and related equipment were replaced by the Nanoscope-IV version. The upgrade provides several new capabilities, including the ability to collect images up to 4096 x 1024 pixels, which constitutes an improvement of 16 times the previous version; the ability to

control the quality factor for resonating cantilevers for intermittent and non-contact AFM measurements; and improved image processing capabilities.

An automated system to measure fundamental hydraulic properties of soil was designed and constructed for the measurement of capillary pressure–saturation relationships.

An automated system to control flow by hydraulic head was designed and constructed. This new capability enables more precise setup of flow fields via differences in hydraulic head, setup of both saturated and unsaturated (vadose zone) systems, and the ability to conduct experiments with a fluctuating water table. The new computer-controlled system allows for the fluctuation of the water table in way that more closely mimics a natural system.

A Spectra-Physics Nd:YAG-pumped master optical parametric oscillator laser was moved from PNNL's 331 Building into EMSL's Environmental Spectroscopy Laboratory. While this laser belongs to PNNL's Fundamental Science Directorate's Chemical Sciences Division, it will be available to EMSL users using the induced-time-resolved fluorescence spectroscopy system, as well as for the development of a laser-induced breakdown spectroscopy capability.

Future Directions

Three-Dimensional Laser Confocal Microscope. This instrument was obtained to expand the ambient pressure/environmental imaging capabilities within the ES&B Facility. The instrument will seamlessly integrate with the recently upgraded scanning probe microscopy capabilities and utilize the expertise of our resident users to develop this system for research in biogeoscience. This system will be extremely valuable for characterizing protein-protein interaction, bio-mineralization, mineral-microbe interactions *in vivo*, specifically how biomolecules (such as cytochromes) interact with metal ions and minerals (e.g., iron oxides) to perform such tasks as conformation transformation and electron transfer. It will help characterize the diffusion of redox processes involved in bioremediation of contaminated porous minerals.

Applied Field Mössbauer. Now that we have established EMSL as a major Mössbauer center of research in the biogeochemistry arena, expansion of the capability to include applied-field (magnetic) Mössbauer spectrometry is warranted in order to continue to provide state-of-the-art capabilities and expertise to the user community. In general, applied-field (magnetic) Mössbauer spectroscopy would be a useful complementary tool for identification and characterization of various Fe compounds and thus would be valuable to existing and future EMSL users.

Infrared Diode Array Detector. We have established EMSL as a major center for time-resolved, laser-induced fluorescence spectroscopy (TRLFS) and imaging spectromicroscopy (TRLFISM). We have extensive experience in R&D using TRLFS, TRLFISM, and ultrafast laser spectroscopy and their applications in chemical, biological, and geological sciences, including subsurface sediments and natural minerals containing actinides and lanthanides. We will purchase an infrared closed-circuit digital camera in order to extend these capabilities into the infrared region.

Laser-Induced Breakdown Spectroscopy and Detection (LIBS/LIBD). The intrinsic similarities between LIBS/LIBD techniques and laser-induced fluorescence techniques along with the fast laser systems and detection systems we currently have in EMSL offer a unique advantage and starting point to develop the LIBS/LIBD capabilities. The camera will also be used to develop laser-induced breakdown spectroscopy/detection capabilities for the investigation, detection, and quantitative analysis of environmentally important toxic metals, such as chromium, lead, arsenic, and sulfur as well as the detection of actinide-bearing aerosols and solid particles and nanocolloids *in situ*.

Electron Microscopy Evaluation of the Role of Dissimilatory Metal-Reducing Bacteria in Biomineralization Pathways

A Dohnalkova,^(a) CM Hansel,^(b) YA Gorby,^(a) and S Fendorf^(b)

(a) Pacific Northwest National Laboratory, Richland, Washington

(b) Stanford University, Stanford, California

The interaction of metal-reducing microorganisms with mineral surfaces such as iron oxides is one of the most complex and important reactions in nature. Use of electron microscopies allows investigation of mineral association with bacterial cells, crystal size, morphology, and spatial relationships. Understanding these processes may lead to improvements in bioremediation processes.

The importance of microorganisms in the biogeochemical cycling of iron is well recognized. Dissimilatory metal-reducing bacteria, which are ubiquitous in soils and aquifers, couple the oxidation of organic matter or hydrogen with the reduction of various Fe(III) oxide phases to obtain energy for growth and function. They can also catalyze Fe(III) reduction under anaerobic conditions, using crystalline and poorly crystalline iron oxides as a terminal electron acceptor.

Microbially induced iron mineral transformations were examined using *Shewanella putrefaciens*, strain CN32, in an artificial groundwater medium in columns under advective flow conditions (Hansel et al. 2003) (Figures 1a and 1b). In this experiment, columns were filled with ferrihydrite-coated quartz sand inoculated with *S. putrefaciens* (initial cell density 108/mL). Lactate was added as an electron donor. Changes in microbial metabolism, aqueous chemistry, and solid-phase distributions were then monitored at time points until termination of the column experiment at 16 days.

Transmission electron microscopy (TEM) and scanning electron microscopy (SEM) were used to investigate mineral association with bacterial cells, crystal size, morphology, and spatial relationships. A special EMSL-developed TEM sample preparation protocol was used for the accurate preservation of both the biological and mineral portions of the sample. To eliminate exposure of the anaerobic sample to oxygen, the entire embedding procedure, as well as the thin sectioning on an ultramicrotome, was carried out in an anaerobic glove box (95 percent argon, 5 percent hydrogen). Ultrathin sections of the material were studied using a JEOL 2010 TEM operating at 200 kV coupled to an Oxford Instruments energy-dispersive spectroscopy system. Images were collected and analyzed using a Digital Micrograph (Gatan), with selected area diffraction patterns evaluated by Desktop Microscopist (Lacuna) software.

Visual changes in the solid phase within the column were evident: as the ferrihydrite, which was initially orange in color, was converted to predominantly goethite and magnetite, it turned brown and further darkened over the course of the experiment (Figures 1c and 1d).

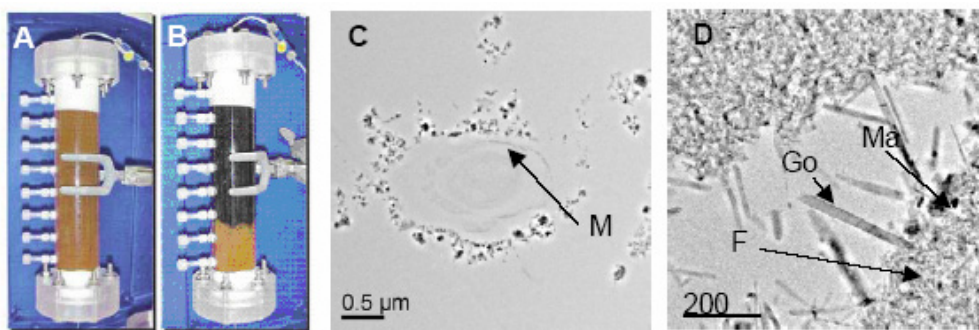


Figure 1. Bacterially assisted mineral transformation of ferrihydrite-coated sand in advective flow columns. A: Ferrihydrite at the starting point. B: After 16 days of reduction, magnetite was the dominant phase. C: Unstained cross section of secondary minerals surrounding bacterial cell. Membrane (arrow). D: Goethite needle-like crystals (Go), magnetite (Ma), nanocrystalline ferrihydrite (F). Scale bar is 200 nanometers.

In addition to spectroscopic methods, the presence of goethite and magnetite was further confirmed by TEM and SEM, and the spatial orientations and size of mineral particles were determined. Typical needle-like structures of goethite crystals were predominantly associated with the surface of ferrihydrite but were also found coupled with microbial cell surfaces. In fact, some bacterial cells appeared completely encrusted in goethite, most likely a result of electrostatic attraction between newly precipitated goethite and the microbial surface. Magnetite, on the other hand, was mainly associated with the ferrihydrite surface, and only rarely with the cell surface. Thus, the bacterial cell is only indirectly (by ferrous iron production) responsible for goethite and magnetite formation. Although intracellular precipitation of iron oxides in *S. putrefaciens* was recently reported (Glasauer et al. 2002), only extracellular precipitation was observed in this experimental setup. Bacteria have the ability to shed the mineral deposits from their outer membranes in order to prevent surface passivation caused by mineral sorption. Bacteria appeared to primarily serve as an Fe(II) source for the system; secondary mineralization was confirmed as a function of initial Fe(II) concentrations.

The mechanism of enzymatic reduction is not completely understood, and the accountable protein functions are being intensively investigated using several molecular biology techniques. Current and future studies will include immunogold labeling at the electron microscopy level as a method for determining localization of these proteins.

Citations

Glasauer S, S Langley, and TJ Beveridge. 2002. "Intracellular Iron Minerals in a Dissimilatory Iron-Reducing Bacterium." *Science* 295(5552):117-119.

Hansel CM, SG Benner, J Neiss, A Dohnalkova, RK Kukkadapu, and S Fendorf. 2003. "Secondary Mineralization Pathways Induced by Dissimilatory Iron Reduction of Ferrihydrite under Advective Flow." *Geochimica et Cosmochimica Acta* 67(16):2977-2992.

Bacterial Nanowires: A Novel Mechanism for Extracellular Electron Transfer

YA Gorby,^(a) A Dohnalkova,^(a) KM Rosso,^(a) S Yanina,^(a) AS Beliaev,^(a) JS McLean,^(a) and JK Fredrickson^(a)

(a) Pacific Northwest National Laboratory, Richland, Washington

Metal-reducing bacteria produce electrically conductive appendages (bacterial nanowires) when limited for terminal electron acceptors. This discovery, which fundamentally transformed our understanding of electron transfer reactions facilitated by bacteria, resulted from combining microscopic and spectroscopic technologies available within the W.R. Wiley Environmental Molecular Sciences Laboratory and controlled cultivation technologies available at PNNL's Microbial Cell Dynamics Laboratory.

Shewanella oneidensis strain MR-1 and other dissimilatory metal-reducing bacteria share the challenge of dealing with reactants and products of respiration that are in the solid phase. While these organisms use a wide range of electron acceptors that are soluble species before and after reduction, they also reduce several metals such as iron or manganese that exist predominantly as oxides or oxyhydroxides. At neutral pH, the solubility of these phases is exceedingly low and the metal ions are poorly available as electron acceptors. We determined that *S. oneidensis* strain MR-1 cells produce extracellular appendages in response to electron acceptor limitation in continuous cultures.

We analyzed *S. oneidensis* MR-1 growing in well-defined continuous cultures (chemostats) with electron acceptor limitation using oxygen as the terminal electron acceptor. Under these conditions, cultures consisted of aggregates of cells with fiber-like appendages ranging from 50 to >150 nm in diameter and as long as tens of microns (Figure 1, top). These appendages were examined by scanning tunneling microscopy (STM) in air to assess their electrical character. STM is a scanning probe technique that entails detection of a tunneling current passing between a sample electrically biased against an atomically sharp metal tip.

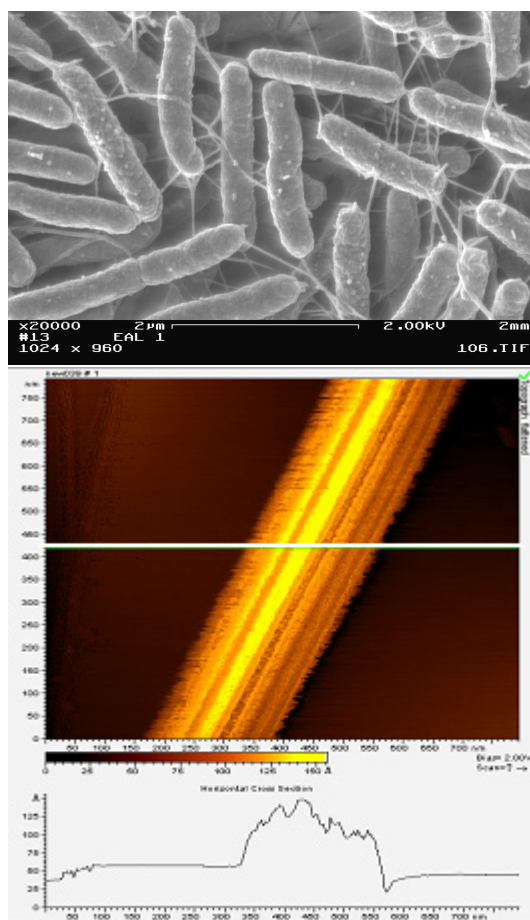


Figure 1. Top: scanning electron microscopy (SEM) image of wild-type strain MR-1 taken from an electron acceptor limited chemostat operating at low agitation (50 rpm). Bottom: STM image of an isolated appendage from wild-type MR-1, with lateral diameter of 100 nm and a topographic height between 5 and 10 nm. Note the ridges and troughs running along the long axis of the structures.

For conducting samples, this is a non-contact technique, with tip-sample distances on the order of a few Ångstroms. Appendages from MR-1 cells grown under electron acceptor limitation were applied to a freshly cleaved surface of highly ordered pyrolytic graphite (an STM standard flat conducting substrate) and thoroughly washed with anaerobic solution of phosphate buffered saline followed by anaerobic deionized water to remove salts present in the medium.

High-resolution STM images (constant current topographs) of isolated appendages on the graphite surface revealed their widths to range from approximately 5 to 100 nm (Figure 1, bottom), consistent with dimensions observed by SEM and atomic force microscopy. The apparent heights of the appendages in the STM images were approximately 10 nm (Figure 2, bottom). At these length scales, height information from STM depends on sample conductivity as well as actual dimensions. For conducting appendages, the substrate bias voltage is carried from the graphite through the appendage. Hence, the bias voltage drop occurs at the upper surface of the appendage and the tip effectively follows the appendage topography. For poorly conducting appendages, the voltage drop is entirely at the graphite surface; hence, the tip seeks the tunneling current from the graphite alone and is effectively blind to the appendage in between. Intermediate conditions may also exist. In our case, all evidence suggests that these appendages are good electrical conductors.

We investigated components of bacterial nanowires using mutants rationally chosen from previously published data implicating the role of outer membrane cytochromes in the reduction of iron and manganese oxides. We constructed an in-frame dilution mutant of *mtrC* (*omcB*, SO1778), $\Delta mtrC$, which encodes a decaheme c-type cytochrome that has been reported to be localized to the outer membrane and necessary for iron reduction *in vivo*. SEM revealed that this mutant produced structures (Figure 2, top) with similar physical dimensions as those nanowires produced by wild-type MR-1. However, the STM apparent heights of the $\Delta mtrC$ mutant appendages (Figure 2, bottom) were almost two orders of magnitude less than for the wild-type appendages, indicating that the appendages produced by this mutant were significantly poorer electrical conductors than MR-1. Notably, this

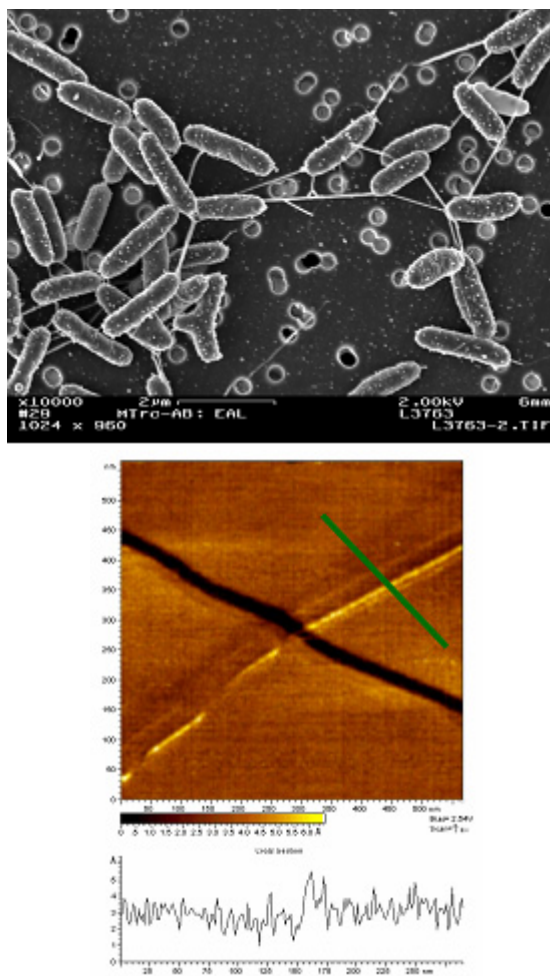


Figure 2. Top: SEM image of $\Delta mtrC$ cultivated under electron acceptor limited conditions. Bottom: STM image of nanowire produced by $\Delta mtrC$, revealing a poorly conductive nature of this structure.

mutant, as well as other mutants that formed non-functional nanowires, was unable to reduce solid-phase iron oxides.

Our findings provide important insights into the mechanisms of electron transfer of metal-reducing bacteria to iron and manganese oxides and perhaps in complex three-dimensional communities such as biofilms.

Electron Transfer Properties of OmcA, an Outer Membrane Decaheme Cytochrome from the Dissimilatory, Metal-Reducing Bacterium *Shewanella oneidensis*

NS Wigginton,^(a) MF Hochella, Jr.,^(a) KM Rosso,^(b) BH Lower,^(b) and L Shi^(b)

(a) Virginia Polytechnic Institute and State University, Blacksburg, Virginia

(b) Pacific Northwest National Laboratory, Richland, Washington

Electron transfer reactions at the mineral-microbe interface can significantly control biogeochemical cycling of metals in the environment. These reactions are thought to be mediated by the direct interaction of specific bacterial outer membrane proteins with mineral surfaces. Expanding knowledge of these processes may aid in the development of potential bioremediation strategies for the cleanup of heavy metals and radionuclides.

Cytochromes are enzymes that function in respiration and photosynthesis processes by transferring electrons across a gradient or membrane. Within individual molecules, electrons are shuttled through iron centers in prosthetic heme groups (iron clusters) within the protein framework via a reversible change in oxidation state. Dissimilatory metal-reducing bacteria are hypothesized to use outer membrane cytochromes such as OmcA as primary catalysts for the terminal transfer of electrons into the crystal structure of Fe(III)- and Mn(IV)-oxide mineral surfaces. Using scanning tunnel microscopy (STM) and scanning tunneling spectroscopy, this study aims to provide a new understanding of the molecular electron-transfer properties of OmcA, a surface-exposed decaheme cytochrome from the bacterium *Shewanella oneidensis*.

OmcA was purified according to previous protocol (Shi et al. 2005). Using a Pico SPM controller and 300S-type scanner (Molecular Imaging, Inc.), ambient STM imaging of OmcA—covalently bonded to atomically flat Au (111) films via thiol groups by a tetra-cysteine tag—show a relatively homogeneous monolayer (Figure 1). In some cases, there appears to be a bias-dependent conductivity of the cytochromes, but more work is required to fully describe this phenomenon. Future studies using *in situ* STM in solution are planned to further our understanding of these observations. Regardless, stable images in air were collected in constant-current mode over repetitive scans once imaging conditions were optimized.

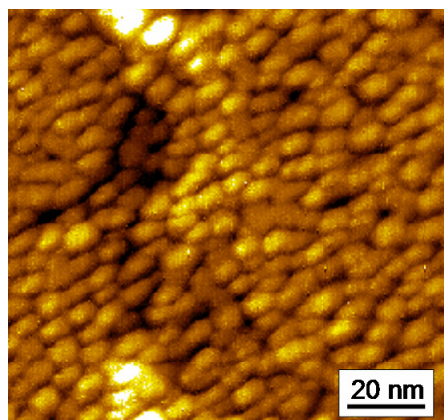


Figure 1. STM image of immobilized OmcA on Au(111) terraces. The uniform size and shape of the cytochrome molecules suggest homogenous distribution and mono-layer coverage as well as consistent protein folding. Scan conditions were 1.08V and 0.5nA in constant current mode.

In addition to imaging, a key component of the STM is that it allows for simultaneous spectroscopic analysis. After the tip is centered over a certain point—in this case, an individual protein molecule—the feedback loop is briefly turned off and the tunneling current (I) is recorded as a function of applied bias voltage (V) swept over a wide voltage range. Several hundred $I(V)$ curves were averaged over multiple protein molecules on various different protein films (Figure 2A). The averaged data were then fit to a modified Simmons equation for direct tunneling (Zhao et al. 2004) (Figure 2B) using non-linear regression analysis. Both Au (111) and OmcA tunneling data fit very well to the model, which suggests that direct tunneling is occurring through the cytochromes within the molecular junction. Previously unknown tunneling parameters for OmcA and Au (111) were then projected from the Simmons equation (Figure 2C).

In direct comparison, the difference in barrier height and width between clean Au(111) surfaces and OmcA suggests tunneling between the STM tip and gold was enhanced by the presence of OmcA. Additional studies of other decahemes cytochromes, including MtrA and MtrC, will provide comparable quantitative information specific to different cytochromes in the electron transport chain. With this and other complementary knowledge in collaboration with EMSL's Biogeochemistry Scientific Grand Challenge, we may have a better understanding of cytochrome-mediated electron transfer reactions that occur at the mineral-microbe interface.

Citations

Shi L, JT Lin, LM Markillie, TC Squier, and BS Hooker. 2005. "Overexpression of Multi-Heme C-Type Cytochromes." *Biotechniques* 38(2):297-299.

Zhao J, JJ Davis, MSP Sansom, and A Hung. 2004. "Exploring the Electronic and Mechanical Properties of Protein Using Conducting Atomic Force Microscopy." *Journal of the American Chemical Society* 126(17):5601-5609.

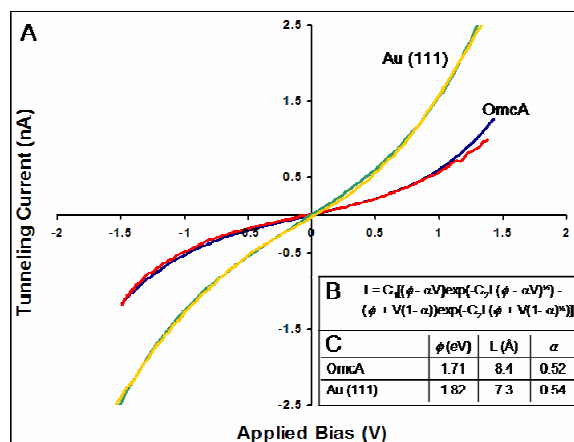


Figure 2. A: Representative experimental $I(V)$ curves for gold (yellow) and OmcA (red) plotted against best-fit curves obtained by non-linear regression analysis. B: Modified Simmons formula used to model experimental data. C: Tunneling parameters for gold and OmcA obtained by solving the Simmons formula using the best-fit curves of the experimental data. The parameters are barrier height (ϕ), barrier width (L), and a voltage-ratio parameter (α).

Kinetic Evidence for Five-Coordination in $\text{AlOH}_{(\text{aq})}^{2+}$ Ion

TW Swaddle,^(a) J Rosenqvist,^(b) P Yu,^(b) EJ Bylaska,^(c) BL Phillips,^(d) and WH Casey^(b)

(a) University of Calgary, Calgary, Alberta, Canada

(b) University of California, Davis, California

(c) Pacific Northwest National Laboratory, Richland, Washington

(d) State University of New York, Stony Brook, New York

Determination of the structure of aluminum in solution in the critical biochemical and geochemical range pH 4-7 is important because its chemical properties, such as aqueous speciation and ligand substitution kinetics, govern aluminum's toxicity towards plants, fish, and humans.

Aluminum ions are important in natural bodies of water because of their potential health effect on plants and fish, but the structure of their coordination shell is a complex, unsolved problem. In strong acid (pH <3.0), Al-III exists almost entirely as the octahedral $\text{Al}(\text{H}_2\text{O})_6^{3+}$ ion, whereas in basic conditions (pH >7), a tetrahedral $\text{Al}(\text{OH})_4^-$ structure prevails. In the biochemically and geochemically critical pH range of 4.3 to 7.0, the ion structures are less clear. Other hydrolytic species, such as $\text{AlOH}_{\text{aq}}^{2+}$, exist and are traditionally assumed to be hexacoordinate.

High-pressure ^{17}O -nuclear magnetic resonance (obtained at the University of California, Davis, and State University of New York, Stony Brook) showed, however, that the kinetics of proton and water exchange on aqueous Al-III, coupled with Car-Parrinello simulations performed using the W.R. Wiley Environmental Molecular Sciences Laboratory's 11.8-teraflop supercomputer, supported a five-coordinate $\text{Al}(\text{H}_2\text{O})_4(\text{OH})^{2+}$ ion as the predominant form of $\text{AlOH}_{(\text{aq})}^{2+}$ under ambient conditions (Figure 1). This result contrasts Al-III with other trivalent metal aqua ions, for which there is no evidence for stable pentacoordinate hydrolysis products.

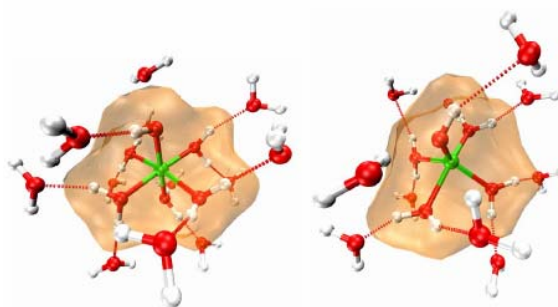


Figure 1. Snapshot of the initial $\text{Al}(\text{H}_2\text{O})_6^{3+}$ geometry (left) and the five-coordinate AlOH^{2+} ion (right) that forms in the Car-Parrinello molecular dynamics simulations.

This work is further described in Swaddle et al. 2005.

Citation

Swaddle TW, J Rosenqvist, P Yu, E Bylaska, BL Phillips, and WH Casey. 2005. "Kinetic Evidence for Five-Coordination in $\text{AlOH}_{(\text{aq})}^{2+}$ Ion." *Science* 308(5727):1450-1453.

Reoxidation of Reduced Uranium with Iron(III) (Hydr)Oxides under Sulfate-Reducing Conditions

RK Sani,^(a) BM Peyton,^(a) A Dohnalkova,^(b) and JE Amonette^(b)

(a) Washington State University, Pullman, Washington

(b) Pacific Northwest National Laboratory, Richland, Washington

Thousands of sites across the United States contain high levels of uranium contaminants generated by mining and processing activities. Understanding uranium precipitation by metal-reducing bacteria may lead to improvements in bioremediation processes.

Uranium is the most common radionuclide in soils, sediments, and groundwater at U.S. Department of Energy sites across the nation and therefore is of particular environmental concern. The most common form of uranium in groundwater is typically U(VI), which is present either as the uranyl cation, schoepite, or as anionic carbonate complexes. Removal of U(VI) from solution can occur by sorption, precipitation as a U(VI) compound, or reductive precipitation as a U(IV) compound. Although sorption of U(VI) can control aqueous concentrations of uranium under oxidizing conditions, the reversibility of such a process makes reductive precipitation more desirable. *In situ* microbial reduction of U(VI) to form U(IV) precipitates of uraninite may be an attractive alternative strategy for remediation of uranium-contaminated subsurface environments. It is vital, therefore, to identify and characterize processes that control the stability of uranium to restrict its environmental risk.

Knowledge of U(VI) reduction by sulfate-reducing bacteria under microbial growth conditions is limited. *In situ* stimulation of anaerobic microbial metal-transformation processes may be an effective treatment alternative to immobilize heavy metals and radionuclides. More research is needed, however, to better understand interactions of sulfate-reducing bacteria, metal, radionuclide contaminants, and mineral phases in the subsurface.

X-ray absorption near-edge spectroscopy performed at Argonne National Laboratory and high-resolution transmission electron microscopy performed at W.R. Wiley Environmental Molecular Sciences Laboratory were used to analyze microbially reduced uranium particles. The results provide evidence that *Desulfovibrio desulfuricans* G20 reduced U(VI) to form nanoparticulate uraninite (Figure 1). Further, results indicate that the type and amount of iron(III) (hydr)oxide present and the type of pH buffer (PIPES or bicarbonate) had significant effects on the rate of U(VI) reduction. After

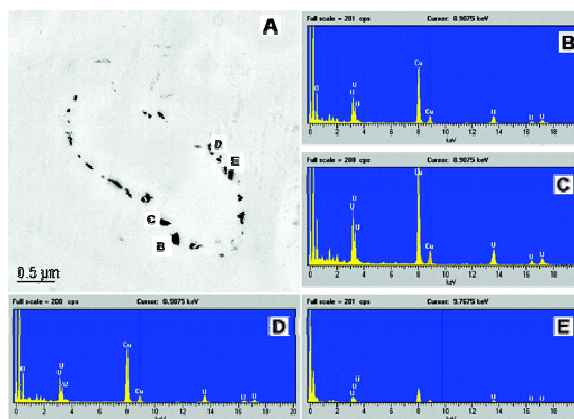


Figure 1. A: Transmission electron microscopy image of an unstained thin section of *D. desulfuricans* G20 treated with U(VI) and hematite showing an oblique section of a bacterium. B-E: Evident precipitates of biogenic uraninite associated with the cell surfaces were confirmed by energy-dispersive spectroscopy and selected area electron diffraction.

depletion of lactate required for microbial U(VI) reduction, the rate and extent of U(IV) reoxidation were dependent on the type and amount of iron(III) (hydr)oxide present. These results suggest that application of long-term bioimmobilization of uranium must consider additional complexity in processes and reactions because sulfate and sulfate-reducing bacteria are commonly found in many uranium-contaminated aquifers. Failing to maintain sufficient organic substrate concentrations until available Fe(III) is reduced could lead to unfavorable consequences for the long-term stability of immobilized uranium.

This research is further described in Sani et al. 2005.

Citation

Sani RK, BM Peyton, A Dohnalkova, and JE Amonette. 2005. "Reoxidation of Reduced Uranium with Iron(III) (Hydr)Oxides under Sulfate-Reducing Conditions." *Environmental Science and Technology* 39(7):2059-2066.

What is the Fate of N₂ Gas Produced by Microbial Denitrification?

JD Istok,^(a) M Park,^(a) M Oostrom,^(b) and TW Wietsma^(c)

(a) Oregon State University, Corvallis, Oregon

(b) Pacific Northwest National Laboratory, Richland, Washington

(c) W.R. Wiley Environmental Molecular Sciences Laboratory, Richland, Washington

Understanding the fate and transport of nitrogen gas produced in situ by microbial reduction of nitrate is important to evaluating the potential effectiveness of uranium and technetium bioremediation processes.

At the U.S. Department of Energy's Natural and Accelerated Bioremediation Research's Field Research Center at Oak Ridge National Laboratory, researchers are investigating the possibility of using native microbial communities to create anaerobic and reducing conditions that favor the bioreduction of uranium and technetium to their less soluble and mobile forms. However, the high levels of nitrate co-contamination at this site (and many other sites) inhibit microbial uranium and technetium bioreduction. Once nitrate is removed, uranium and technetium reduction occur rapidly. Thus, by stimulating the activity of indigenous denitrifying organisms, nitrate can be reduced to nitrogen allowing metal-reducing organisms to reduce uranium and technetium. However, nitrate concentrations at the site are very large (up to 200 mM), and there is concern that the large quantities of nitrogen gas produced during denitrification will clog the pore space of the treated aquifer. Thus, understanding the fate and transport of nitrogen gas produced *in situ* is important to evaluating the effectiveness of uranium and technetium bioreduction.

To facilitate an understanding of fate and transport of nitrogen gas, a series of experiments at the W.R. Wiley Environmental Molecular Sciences Laboratory (EMSL) were conducted to mimic conditions in the field. A two-dimensional flow cell was packed with a mixture of sediments supplied by the Field Research Facility. The lower half of the flow cell (through port 4) contained sediment from the shallow groundwater aquifer at the site. The upper half (ports 5-8) contained crushed limestone bedrock. Microbial activity was stimulated by a series of electron donor additions similar to those used in field experiments. For each addition, a synthetic groundwater solution amended with 300 mM of ethanol and 150 mM of nitrate was injected into the inlet of the flow cell. Water samples were collected at eight locations within the flow cell and at the outlet. Hydraulic conductivity was measured before and after each ethanol addition. Aqueous and gas-phase saturations were measured using EMSL's dual-energy, gamma-imaging system, and samples were analyzed using ion chromatography and gas chromatography. Successful stimulation of the *in situ* denitrifying microbial community was observed by the consumption of injected ethanol and nitrate, the production of a denitrification by-product (NO₂), and visual observation of gas bubbles in the chamber.

In May 2005, the system was flushed to remove residual ethanol and nitrate, and a test was conducted to quantify rates of ethanol and nitrate consumption, while at the same time quantifying gas production. This test involved injection of a measured quantity of synthetic groundwater prepared as before. Samples were collected and the system was scanned daily

so development of denitrification, production of intermediates, and the extent and location of N_2 gas formation within the pore space could be measured. At the end of the test, the system was destructively sampled to quantify the effects of donor additions on the microbial community.

Figure 1 shows a three-dimensional representation of the flow cell over the course of the 15-day duration of the experiment. Nitrate concentration, initially at ~ 150 mM, was nearly completely reduced in the lower biostimulated portion of the flow cell within about six days. Gas saturation of the pore space rapidly increased and reached a maximum saturation of about 17 percent within the lower portion of the flow cell. Theory predicts that ~ 1.8 L of nitrogen gas will be produced by the complete denitrification of 150-mM nitrate. Measured gas saturations were much smaller, and observations confirm that although substantial gas is produced, only a small portion is trapped within the pore space, while most is released to the sediment pack surface. The effect of gas production on the hydraulic conductivity of the sediment pack was very small. The quantity of organisms produced and the composition of the microbial community is currently being analyzed.

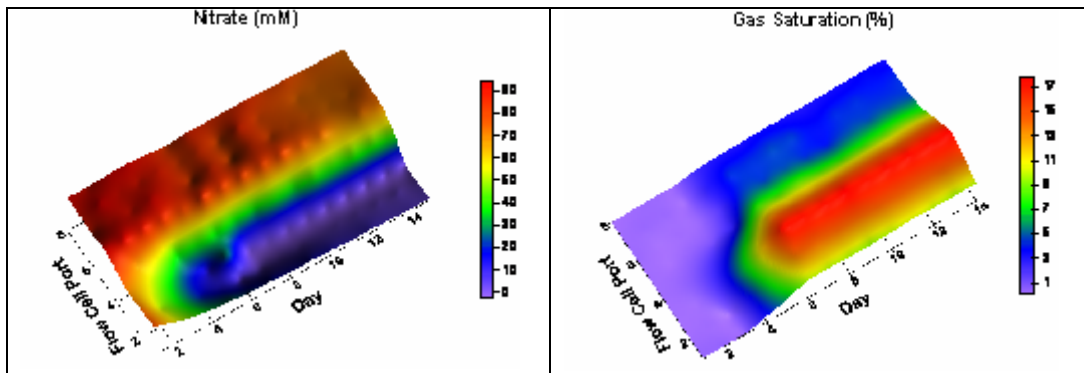


Figure 1. Plot of nitrate concentration and gas saturation (percent) over the course of the 15-day experiment for each of eight ports.

Luminescence from the Trans-Dioxotechnetium(V) Chromophore

A Del Negro,^(a) Z Wang,^(a) CJ Seliskar,^(b) WR Heineman,^(b) BP Sullivan,^(c)
SE Hightower,^(c) TL Hubler,^(a) and SA Bryan^(a)

(a) Pacific Northwest National Laboratory, Richland, Washington

(b) University of Cincinnati, Cincinnati, Ohio

(c) University of Wyoming, Laramie, Wyoming

Subsurface contamination by technetium is of particular concern because of the extremely long life of its most common isotope, ⁹⁹Tc, and the fast migration in soils exhibited by its most common chemical form, pertechnetate. This research contributes to the potential to develop an electrochemical-fluorescence-based sensor to detect technetium in contaminated groundwater at the U.S. Department of Energy's (DOE's) Hanford Site and elsewhere.

Funded by the DOE's Environmental Management Science Program, this research features a collaboration among researchers from the University of Cincinnati (CJ Seliskar and WR Heineman), University of Wyoming (BP Sullivan and SE Hightower), and Pacific Northwest National Laboratory (TL Hubler, SA Byran, A Del Negro, and Z Wang). The work involves the spectroelectrochemical detection of pertechnetate in the vadose zone. Subsurface contamination by technetium is of particular concern because of the extremely long life of its most common isotope, ⁹⁹Tc (half-life = 2×10^5 years), and the fast migration in soils exhibited by its most common chemical form, pertechnetate (TcO₄⁻). A sensor is being designed that has the capability for onsite monitoring, either by immersion in subsurface water for continuous monitoring or for immediate analysis of collected samples. The device combines electrochemistry, spectroscopy, and selective partitioning capabilities, the combination of which substantially improves selectivity.

A Del Negro and Z Wang measured the luminescence and excited-state lifetime properties of a newly discovered Tc(V) chromophore using the W.R. Wiley Environmental Sciences Laboratory liquid helium line-narrowing, laser-induced, time-resolved fluorescence system. Their research has led to the discovery of the first luminescence from trans-dioxo-technetium(V) complexes. The room- and low-temperature luminescence studies of trans-[TcO₂(L)₄]⁺ (L = pyridine or picoline) and trans-[TcO₂(CN)₄]³⁻ opens a new chapter in technetium chemistry, both in a fundamental and practical sense. The low-temperature luminescence spectrum (Figure 1) for

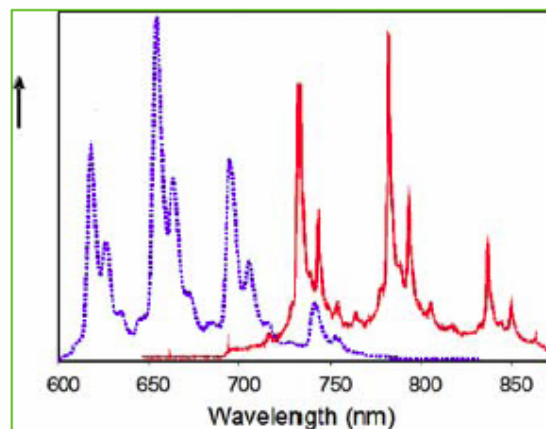


Figure 1. Low-temperature (8 K) luminescence spectra of microcrystalline [ReO₂(pic)₄](BPh₄) (blue) and [TcO₂(pic)₄](BPh₄) (red). Spectra are not normalized for excitation intensity differences.

[TcO₂(pic)₄](BPh₄), with [ReO₂(pic)₄](BPh₄) shown as an overlay spectrum, clearly shows a lower-energy (~180-200 cm⁻¹) vibronic progression for analogous rhenium and technetium complexes. This important development allows the researchers to develop a theoretical model that can be used to predict the optical behavior of technetium complexes in general.

This discovery also provides the first opportunity to directly compare fundamental luminescence properties of second- and third-row d2 metal-oxo congeners. Analytical applications of the TcO₂ chromophore offer promise for design of dual-mode complexes that can correlate luminescence and radioimaging properties into a single agent. For the project's purposes, luminescent Tc(V) complexes are a significant advance in the team's design of a spectroelectrochemical sensor for detection of pertechnetate in the environment.

Measurements to determine quantum yield and absorption spectral data as well as detailed studies of the temperature-dependence of the photophysical properties of the technetium complexes are currently underway.

Electron Density Distributions Calculated for the Nickel Sulfides Millerite, Vaesite, and Heazlewoodite and Nickel Metal: A Case for the Importance of Ni-Ni Bond Paths for Electron Transport

GV Gibbs,^(a) RT Downs,^(b) CT Prewitt,^(b) KM Rosso,^(c) NL Ross,^(a) and DF Cox^(a)

(a) Virginia Polytechnic Institute and State University, Blacksburg, Virginia

(b) University of Arizona, Tucson, Arizona

(c) Pacific Northwest National Laboratory, Richland, Washington

Establishing the relationship between the crystal structure and physical properties of nickel sulfide ores leads to a better understanding of acid mine drainage reactions that may occur in the environment.

Metal sulfides are an important class of ore minerals (Figure 1) that display a host of interesting bonded interactions and structure types in concert with an assortment of important electronic and magnetic properties. These properties have attracted the attention of solid-state physicists, material scientists, and mineralogists who have determined the crystal and electronic structures for a variety of sulfide minerals and representative clusters. Despite the important information provided by these studies, the understanding of the bond length and bond strength variations, bonded interactions, and the structures of a variety of sulfides is lacking, particularly when contrasted with that of the oxides. This shortcoming has been ascribed to the diversity of metal-metal and sulfur-sulfur bonded interactions displayed by a number of sulfides together with traditional metal-sulfur bonded interactions displayed by these and others. This is in contrast with the oxide minerals for which only metal-oxygen interactions are displayed.

This collaboration and the resulting publication (Gibbs et al. 2005) focused on improving the understanding of how the electrical properties of nickel sulfide minerals arise from their structures. The strategy taken involves computation of the electron density along all possible interatomic paths in their crystal structures. Where the electron density is found to be locally maximal in two dimensions perpendicular to the interatomic path and locally minimal in the direction along the interatomic path, this is taken as direct evidence of a bonded interaction between the two atoms. By seeking bond paths and characterizing the electron density along the bond paths, we have categorized the bond types and numbers in each structure. Contiguous M-M bond

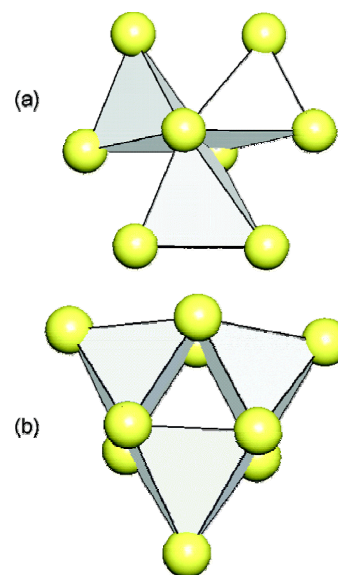


Figure 1. Polyhedral drawings of the (a) Ni_3S_8 cluster in heazlewoodite and the (b) Ni_3S_9 cluster in millerite. The large spheres represent sulfur. The nickel atoms are not displayed but are enclosed within the polyhedra. The nickel atoms are coordinated by four sulfur atoms disposed at the corners of a distorted tetrahedron in heazlewoodite and by five sulfur atoms disposed at the corners of a square pyramid in millerite.

paths are found in the structures that are electrical conductors, even if metal-metal distances are longer than in non-conducting structures. The calculations required treatment at the density functional level of theory and were performed on the W.R. Wiley Environmental Molecular Sciences Laboratory supercomputer using the quantum mechanical codes Crystal98 and Topond98.

Citation

Gibbs GV, RT Downs, CT Prewitt, KM Rosso, N Ross, and DF Cox. 2005. "Electron Density Distributions Calculated for the Nickel Sulfides Millerite, Vaesite, and Heazlewoodite and Nickel Metal: A Case for the Importance of Ni-Ni Bond Paths for Electron Transport." *Journal of Physical Chemistry B* 109(46):21788-21795.

The Influence of Edge Sites on the Development of Surface Charge on Goethite Nanoparticles: A Molecular Dynamics Investigation

JR Rustad^(a) and AR Felmy^(b)

(a) University of California at Davis, Davis, California

(b) Pacific Northwest National Laboratory, Richland, Washington

Understanding the basic reaction of a mineral surface with hydrogen ions is the basis for elucidating the rest of the mineral's chemical behavior. Understanding these chemical and physical processes is important in determining the fate and transport of chemicals in the environment and may lead to the development of more efficient remediation technologies.

The extent of protonation of oxide surfaces has a fundamental influence on virtually every aspect of their chemical behavior in aqueous systems, governing dissolution/precipitation, sorption, and redox reactions and controlling the mobility and aggregation state of colloidal-sized particles. Much attention has been focused in the literature on relating proton surface charging to oxide surface structure. The current intellectual framework for progress in understanding mineral surfaces reactivity has been built on a series of well-defined systems of increasing complexity. For the oxides, a systematic path starts by investigating surfaces in vacuum environments and attempting to relate ultrahigh vacuum surface structures to bulk structures. These surfaces are then exposed to small amounts of water to ascertain the extent of dissociation and binding energies. Solvated surfaces are then studied with surface-sensitive, x-ray-scattering techniques. At each level, information is fed upwards. Computational methods have been useful in amalgamating experimental results making up this framework.

Real surfaces are, of course, never ideal, and recent studies have emphasized the relationship between structural and energetic heterogeneity in complex environments. On sufficiently small scales, surface-surface interactions may alter the patterns of reactivity expected for idealized interfaces. In our paper (Rustad and Felmy 2005), molecular dynamics simulations were used to compute proton distributions on faceted goethite particles 3 to 8 nm in size. The major finding is that, at these length scales, the simulated proton distributions do not at all reflect the sum of contributions from individual crystal faces. Instead, protons accumulate preferentially at edge regions that are defined by the acute intersections of (110)-(110) surfaces.

Although there are several possible explanations for this behavior (Figure 1), we ascribe the effect to the more effective salvation of excess charge at the acute edges. This pattern of charge development is proposed to influence the thermodynamics and kinetics of acid-base, surface complexation, and oxidation-reduction reactions in these systems.

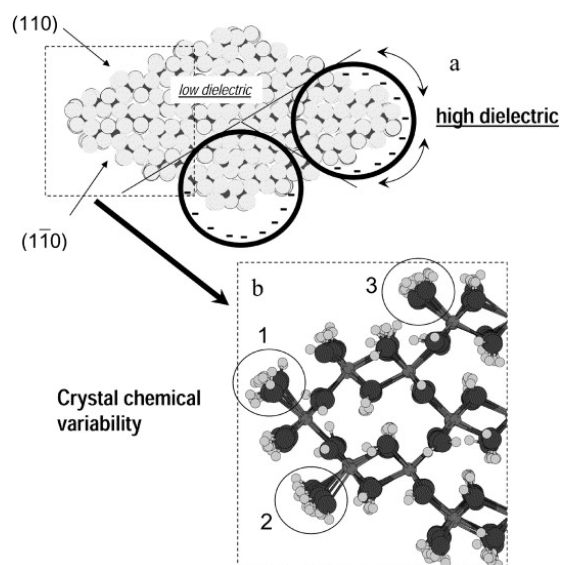


Figure 1. Possible reasons for the inhomogeneous proton charge accumulation on the surfaces of the nanoparticles: a) dielectric effects allowing more effective solvation of excess positive charge at acute edge sites; b) crystal chemical variability in circled FeO sites due to finite size of particle; and 3) an Fe³⁺ OH site underlies the circled FeO site. Such underlying sites are absent in 1) and 2), presumably increasing their proton affinities. Mechanism a) should show up as an increase in proton uptake, but will have little effect on the zero point of charge; whereas mechanism b) will shift the zero point of charge in the direction of increasing pH.

Citation

Rustad JR and AR Felmy. 2005. "The Influence of Edge Sites on the Development of Surface Charge on Goethite Nanoparticles: A Molecular Dynamics Investigation." *Geochimica et Cosmochimica Acta* 69:1405-1411.

Dissolution of Uranyl Microprecipitates in Subsurface Sediments at the Hanford Site

C Liu,^(a) JM Zachara,^(a) O Qafoku,^(a) JP McKinley,^(a) SM Heald,^(b) and Z Wang^(a)

(a) Pacific Northwest National Laboratory, Richland, Washington

(b) Argonne National Laboratory, Argonne, Illinois

Because of its central role in the nuclear fuel cycle, uranium is a common subsurface contaminant at U.S. Department of Energy (DOE) sites. Understanding the chemical and physical behavior of uranium is important in determining the fate and transport of chemicals in the environment and may lead to the development of more efficient remediation technologies.

The geochemical behavior of uranium, including its reactive transport chemistry and potential for remediation, is a matter of concern and intensive research. Subsurface uranium mobility is controlled by adsorption to mineral materials and dissolution/precipitation of uranium solids. Uranium is hexavalent [U(VI)] under oxidized conditions and exists as the uranyl ion (UO_2^{2+}) and its complexes with various ligands in the aqueous phase.

In our paper (Liu et al. 2004), the rate and extent of uranyl dissolution was measured from three Hanford Site vadose zone sediments that had been contaminated by a high-level nuclear waste discharges more than 50 years ago. The uranium in the sediments exists as discontinuous particle coatings and intragrain precipitates of uranyl silicates, primarily in plagioclase-containing clast fragments. Our objective was to quantify the physical, mineralogical, chemical, and thermodynamic factors controlling uranium release to the aqueous phase. Dissolution was studied over a range of pH levels and electrolyte concentrations representative of the calcareous geochemical environment from which the samples were obtained. A kinetic model involving carbonate-mediated dissolution kinetics and diffusion from intra-grain fracture domains was developed to provide insights on factors controlling the slow observed release rates and incomplete extent of uranium dissolution from the three sediments.

The dissolution of uranium was investigated from contaminated sediments obtained at DOE's Hanford Site (Figure 1). The uranium existed in the sediments as uranyl silicate microprecipitates in fractures, cleavages, and cavities within sediment grains. Uranium dissolution was studied in sodium, sodium/calcium, and ammonium electrolytes with pH levels ranging from 7.0 to 9.5 under ambient carbon dioxide pressure. The rate and extent of uranium dissolution was influenced by uranyl mineral solubility, carbonate concentration, and mass transfer rate from intra-particle regions. The dissolved uranium concentration reached constant values within a month in electrolytes below pH 8.2, whereas concentrations continued to rise for over 200 days at pH levels of 9.0 and above. The steady-state concentrations were consistent with the solubility of sodium-boltwoodite and/or uranophane, which exhibit similar solubility under experimental conditions. The uranium dissolution rate increased with increasing carbonate concentration and was initially fast. The dissolution rate decreased with time as solubility equilibrium was attained, or dissolution kinetics or mass transfer rate from intra-particle regions became rate-limiting. Microscopic observations indicated that uranium precipitates were distributed in intra-grain

microfractures with variable sizes and connectivity to particle surfaces. Laser-induced fluorescence spectroscopic change of the uranyl microprecipitates was negligible during the long-term equilibration, indicating that uranyl speciation was not changed by dissolution. A kinetic model that incorporated mineral dissolution kinetics and grain-scale, fracture-matrix diffusion was developed to describe uranium release rate from the sediment. Model calculations indicated that 50 to 95 percent of the precipitated uranium was associated with fractures that were in close contact with the aqueous phase. The remainder of the uranium was deeply imbedded in particle interiors and exhibited effective diffusivities that were more than three orders of magnitude lower than those in the fractures.

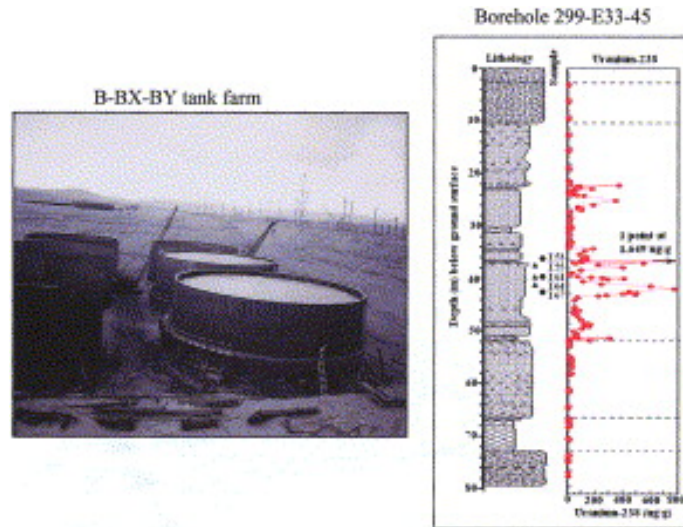


Figure 1. The photograph (left plot) shows the Hanford Site BX tank farm under construction. Tank BX-102 is the middle on the right. The plot (right) shows the distribution of uranium in Borehole 299-E33-45 (near Tank BX-102). The collection depths for the sediment (circle) and pore water (triangle) samples are noted at 35 to 45m. The borehole was located approximately 9 m to the right of BX-102.

Citation

Liu C, JM Zachara, O Qafoku, JP McKinley, SM Heald, and Z Wang. "Dissolution of Uranyl Microprecipitates in Subsurface Sediments at the Hanford Site, USA." *Geochimica et Cosmochimica Acta* 68:4519-4537.

Mica Surfaces Stabilize Pentavalent Uranium

ES Ilton,^(a) A Haiduc,^(b) CL Cahill,^(c) and AR Felmy^(a)

(a) Pacific Northwest National Laboratory, Richland, Washington

(b) Shell Global Solutions International, Amsterdam, The Netherlands

(c) George Washington University and the Carnegie Institution of Washington, Washington, D.C.

Uranium is a common subsurface contaminant at U.S. Department of Energy sites because of its central role in the nuclear fuel cycle. Understanding the chemical and physical behavior of uranium is important in determining its fate and transport of chemicals in the environment. The finding of this study is that pentavalent uranium, U(V), does exist on mineral surfaces and indicates that a key aspect of the cycling of uranium in the environment has been previously overlooked.

Uranium was discovered in 1789, but aqueous U⁵⁺ was not identified until the 1940s during the Manhattan Project. U⁵⁺ in aqueous solution as UO²⁺ has a narrow stability field between pH 2 and 4; outside this pH regime, U⁵⁺ rapidly disproportionates. The initial findings discounted the possibility of U⁵⁺ existing in the environment. E Ilton and co-workers (2005) discovered that heterogeneous reduction of aqueous U⁶⁺ at ferrous mica surfaces produces and preserves U⁵⁺, as a sorbed species, over a broad range of solution compositions.

Macroscopic single crystals of annite, the near-end member ferrous trioctahedral mica, were reacted with argon-sparged aqueous solutions containing 5 μM U⁶⁺ and variable Na⁺ from pH 4.5 to 9.5. X-ray photoelectron spectroscopy (XPS) spectra of the U4f level for uranium sorbed on annite edge orientations were fit with three components representing U⁶⁺, U⁵⁺, and U⁴⁺. XPS yields information on the chemical state and composition of solid surfaces, where most of the signal was integrated over the top 80 Å of our sample. The valence of uranium can be determined from the binding energies and satellite structures associated with the 4f_{7/2} and 4f_{5/2} levels, and the 5f intensity. In 2004, E Ilton and his team demonstrated that structural Fe(II) in micas can reduce sorbed U⁶⁺, but modeled the 4f_{7/2} primary peak with only two components (assumed to be U⁴⁺ and U⁶⁺). Good fits across a wide range of average uranium oxidation states were only possible by not including the satellite structure in the fitting and by allowing wide variations in both the full-width-at-half-maximum and binding energy separation of the component peaks. In their latest work, U⁵⁺ was discovered by explicitly including the satellite structure and three components in fitting the spectra. Schoepite, UO₃·(H₂O)₃, and uraninite, UO₂, were used to derive peak parameters for the U⁶⁺ and U⁴⁺ components. The U⁵⁺ component was derived by fitting a (U⁵⁺-U⁶⁺) oxyhydroxide, synthesized under hydrothermal conditions, with the U⁶⁺ component and solving for the U⁵⁺ peak parameters.

The finding of pentavalent uranium on mineral surfaces indicates that a key aspect of the cycling of uranium in the environment has been previously overlooked. The results show that U⁵⁺ could play an important, but previously unidentified, role in the low-temperature

geochemical cycling of uranium. This research is the cover feature of the May 2, 2005 issue of *Inorganic Chemistry* (Ilton et al. 2005) (Figure 1).

Citation

Ilton ES, A Haiduc, CL Cahill, and AR Felmy. 2005. "Mica Surfaces Stabilize Pentavalent Uranium." *Inorganic Chemistry* 44(9):2986-2988.

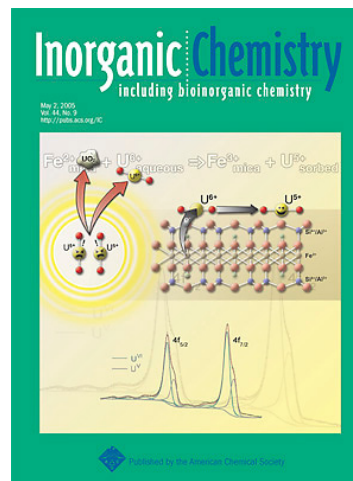


Figure 1. Cover of May 2, 2005, issue of *Inorganic Chemistry*.

Effects of Sediment Iron Mineral Composition on Microbially Mediated Changes in Divalent Metal Speciation: Importance of Ferrihydrite

DC Cooper,^(a) AL Neal,^(b) RK Kukkadapu,^(c) D Brewe,^(d) A Coby,^(e) and FW Picardal^(e)

(a) Geosciences Research, Idaho National Laboratory, Idaho Falls, Idaho

(b) Savannah River Ecology Laboratory, Aiken, South Carolina

(c) W.R. Wiley Environmental Molecular Sciences Laboratory, Richland, Washington

(d) Argonne National Laboratory, Argonne, Illinois

(e) Indiana University, Bloomington, Indiana

The ability to accurately reproduce environmental conditions in laboratory experiments is crucial in elucidating microbe-mineral interactions, which is vital to modeling and enabling bioremediation processes.

Dissimilatory reduction of iron oxide minerals has been documented for a large number of microorganisms in a wide range of environments, and has become recognized as an important constituent of the global carbon and iron cycles. This process has a profound effect on groundwater and sediment geochemistry, and can significantly alter the speciation and mobility of contaminant metals. Many investigations into this phenomenon have examined the ability of dissimilatory metal-reducing bacteria (DMRB) to reduce various crystalline Fe(III) sources. The impact of DMRB activity on sediment mineral composition and metal geochemistry has also been extensively researched. Most of these laboratory investigations use either “standard” or synthetic minerals that artificially constrain the experimental systems and do not reflect the complex mineral composition of natural environments. Thus, there are scant data to allow proper linkage between laboratory experimentation and field observation. Therefore, we examined the effect(s) of complex sediment composition on the geochemical outcome of microbial Fe(III) reduction.

Specifically, this study (Cooper et al. 2005) sought to identify 1) how variable iron oxide composition in a sediment system can affect the way(s) that a system responds to a microbial perturbation (dissimilatory Fe(III) reduction) and 2) how such a response may affect the speciation of divalent metals. Zn(II) was chosen because it is a divalent metal that 1) is not sensitive to redox changes, 2) has an ionic diameter similar to that of iron, 3) is relatively soluble at pH ~7, 4) does not form strong aqueous complexes in “typical” groundwater, and 5) has well-defined adsorption chemistry with a variety of mineral surfaces.

Our experiments with a DMRB (*Shewanella putrefaciens* 200) and a divalent metal (Zn(II)) indicate that while complexity in sediment mineral composition may not strongly impact the degree of “microbial iron reducibility,” it does alter the geochemical consequences of such microbial activity. The ferrihydrite and clay mineral content are key factors. Microbial reduction of a synthetic blend of goethite and ferrihydrite (VHSA-G) carrying previously adsorbed Zn(II) increased both [ZnII -aq] and the proportion of adsorbed Zn(II) that is insoluble in 0.5 M HCl. Microbial reduction of Fe(III) in similarly treated iron-bearing clayey sediment (Fe-K-Q) and hematite sand, which contained minimal amounts of ferrihydrite, had no similar effect. Addition of ferrihydrite increased the effect of microbial Fe(III)

reduction on Zn(II) association with a 0.5 M HCl insoluble phase in all sediment treatments, but the effect was inconsequential in the Fe-K-Q. Zinc k-edge, x-ray absorption spectroscopy data indicate that microbial Fe(III) reduction altered Zn(II) bonding in fundamentally different ways for VHSA-G and Fe-K-Q. In VHSA-G, ZnO₆ octahedra were present in both sterile and reduced samples, with a slightly increased average Zn-O coordination number and a slightly higher degree of long-range order in the reduced sample. This result may be consistent with enhanced Zn(II) substitution within goethite in the microbially reduced sample, though these data do not show the large increase in the degree of Zn-O-metal interactions expected to accompany this change. In Fe-K-Q, microbial Fe(III) reduction transforms Zn-O polyhedra from octahedral to tetrahedral coordination and leads to the formation of a ZnCl₂ moiety and an increased degree of multiple scattering. This study indicates that, while many sedimentary iron minerals are easily reduced by DMRB, the effects of microbial Fe(III) reduction on trace metal geochemistry are dependent on sediment mineral composition.

Citation

Cooper CD, AL Neal, RK Kukkadapu, D Brewe, AJ Coby, and FW Picardal. 2005. "Effects of Sediment Iron Mineral Composition on Microbially Mediated Changes in Divalent Metal Speciation: Importance of Ferrihydrite." *Geochimica et Cosmochimica Acta* 69(7):1739-1759.

Ab Initio Electronic Structure Study of One-Electron Reduction of Polychlorinated Ethylenes

EJ Bylaska,^(a) M Dupuis,^(a) and PG Tratnyek^(b)

(a) Pacific Northwest National Laboratory, Richland Washington

(b) Oregon Health & Science University, Beaverton, Oregon

This study demonstrates that ab initio electronic structure methods can be used to calculate the reaction energetics of a potentially large number of organic compounds in solution, including radical and anionic compounds for which experimental data are unavailable, and can also be used to help identify potentially important environmental degradation reactions.

The widespread use of polychlorinated ethylenes as solvents has resulted in their ubiquitous presence in the environment. Because of their volatility, these toxic compounds are widely dispersed at low concentrations in the atmosphere. In the subsurface, the immiscibility of polychlorinated ethylenes leads to pools and ganglia of nonaqueous-phase liquid below a spill site, which then becomes a source for dissolved-phase contamination that can form a very large plume of contaminated groundwater. This kind of contamination is difficult to remediate using extraction technologies such as conventional “pump and treat”; therefore, there is great interest in *in situ* remediation strategies that degrade polychlorinated ethylenes. Most of these technologies, whether chemical or microbiological, rely mainly on reductive reactions for dechlorination of the contaminants (Figure 1).

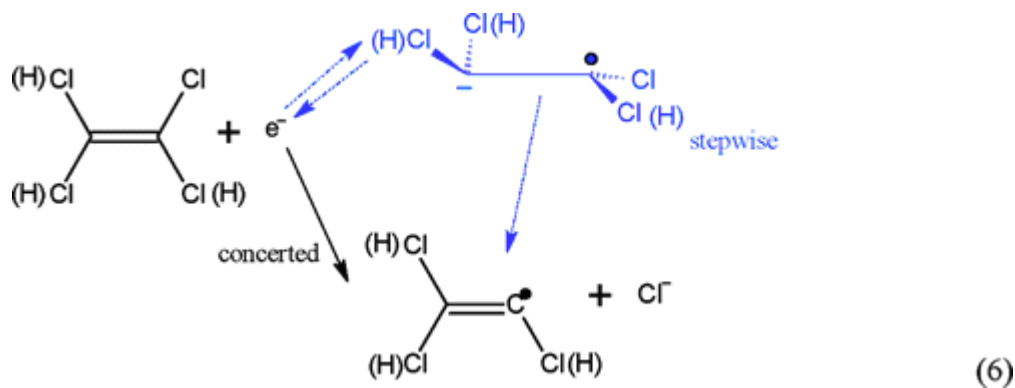


Figure 1. Different reduction pathways.

We have been interested in applying the methods of computational chemistry to study the environmental degradation of simple and larger organo-chlorine compounds. In this study (Bylaska et al. 2005), we used electronic structure methods to investigate the thermochemical properties (in the gas phase and in aqueous solution) for the reaction pathways of polychloroethylenes under reducing conditions. We report thermochemical properties, ΔH_f° (298.15 K), S° (298.15 K, 1 bar), ΔG_s° (298.15 K, 1 bar) calculated throughisodesmic reactions schemes, gas-phase entropy estimates, and continuum solvation models for polychloroethylenyl radicals and anions, and for open-shell polychloroethylene radical anions. From these thermochemical data we estimate the energetics of several one-electron reductive pathways. Our objective is not only to elucidate the specific reaction energetics but also to make inferences on reaction kinetics.

Ab initio electronic structure methods were used to calculate the thermochemical properties, NH_f° (298.15 K), S° (298.15 K, 1 bar), and ΔG_s° (298.15 K, 1 bar), of 37 different polychloroethylenyl radicals, anions, and radical anion complexes, $C_2H_yCl_{3-y}^\bullet$, $C_2H_yCl_{3-y}^-$, and $C_2H_yCl_{4-y}^\bullet$ for $y = 0-3$, for the purpose of characterizing reduction mechanisms of polychlorinated ethylenes. In this study, eight radicals, seven anions, and 22 radical anions were found to have stable structures (i.e., minima on the potential energy surfaces). This multitude of isomers for $C_2H_yCl_{4-y}^\bullet$ radical anion complexes are π^* , σ^* , and $-H \cdots Cl^-$ structures. Several stable π^* radical anionic structures were obtained for the first time through the use of restricted open-shell theories. On the basis of the calculated thermochemical estimates, the overall reaction energetics (in the gas phase and aqueous phase) for several mechanisms of the first electron reduction of the polychlorinated ethylenes were determined. In almost all of the gas-phase reactions, the thermodynamically most favorable pathways involve $-H \cdots Cl^-$ complexes of the $C_2H_yCl_{4-y}^\bullet$ radical anion, in which a chloride ion is loosely bound to a hydrogen of a $C_2H_xCl_{2-x}^\bullet$ radical. The exception is for C_2Cl_4 , in which the most favorable anionic structure is a loose σ^* radical anion complex with a nearly iso-energetic π^* radical anion. Solvation significantly changes the product energetics with the thermodynamically most favorable pathway leading to $C_2H_yCl_{3-y}^\bullet + Cl^-$. The results suggest that a higher degree of chlorination favors reduction, and that reduction pathways involving the $C_2H_yCl_{3-y}^-$ anions are high-energy pathways. Finally, the results of this study demonstrate that *ab initio* electronic structure methods can be used to calculate the reaction energetics of a potentially large number of organic compounds in solution, including radical and anionic compounds for which experimental data are unavailable, and also can be used to help identify the potentially important environmental degradation reactions.

Citation

Bylaska EJ, M Dupuis, and PG Tratnyek. 2005. “*Ab Initio* Electronic Structure Study of One-Electron Reduction of Polychlorinated Ethylenes” *Journal of Physical Chemistry A* 109(26):5905-5916.

User Projects

***Deinococcus radiodurans* for Bioremediation**

Pacific Northwest National Laboratory, Richland, Washington
HM Kostandarithes, JK Fredrickson

Laboratory Studies of Phytoremediation and Apatite Sequestration

Pacific Northwest National Laboratory, Richland, Washington
JL Phillips, JE Szecsody

Formation of Fe(II) Secondary Minerals After Fe(III) Bioreduction in Humid Tropical Forest Soils

University of California, Berkeley, Berkeley, California
T Peretyazhko, G Sposito

Mössbauer Analysis for Goethite Reacted with Fe(II) and Membrane Fraction of *Shewanella oneidensis*

Pennsylvania State University, University Park, Pennsylvania
J Jang

Geochemical Testing and Model Development—Residual Tank Waste

Pacific Northwest National Laboratory, Richland, Washington
KJ Cantrell, WJ Deutsch

Novel Nanoporous Getters to Immobilize ⁹⁹Tc at the Yucca Mountain Waste Repository

Pacific Northwest National Laboratory, Richland, Washington
HM Cho, OS Qafoku, S Mattigod, KM Rosso

Environmental Sensing, Metabolic Response, Regulatory Network

Pacific Northwest National Laboratory, Richland, Washington
JK Fredrickson, DW Kennedy

Proteomics of Bioenergetics

Pacific Northwest National Laboratory, Richland, Washington
J Scholten, DW Kennedy

Low-Cost, Energy-Efficient Nitrogen Fertilizer

Pacific Northwest National Laboratory, Richland, Washington
JE Amonette, CC Bashore

Mechanisms and Dynamics of Abiotic and Biotic Interactions at Environmental Interfaces

Stanford University, Stanford, California

GE Brown

Pacific Northwest National Laboratory, Richland, Washington

KM Rosso, S Yanina

Lignin Content in Natural Fibers Utilizing Fluorescence Microscopy

Pacific Northwest National Laboratory, Richland, Washington

JD Holbery

Theoretical Treatment of the Kinetics of Uranium Reduction by Magnetite Surfaces

State University of New York at Stony Brook, Stony Brook, New York

MC Wander, MA Schoonen, RJ Reeder

Pennsylvania State University, University Park, Pennsylvania

JD Kubicki

Scintillator Research

Pacific Northwest National Laboratory, Richland, Washington

M Bliss, Z Wang

Molecular Forces in Bacterial Adhesion at the Oxide-Water Interface

Virginia Polytechnic Institute, Blacksburg, Virginia

MF Hochella, S Bose, NS Wigginton

Pacific Northwest National Laboratory, Richland, Washington

TC Droubay

Establish a Center for Environmental Kinetics at Pennsylvania State University as Part of the Environmental Molecular Science Institute (EMSI) Program

University of California, Berkeley, Berkeley, California

T Peretyazhko

Pacific Northwest National Laboratory, Richland, Washington

JM Zachara, Z Wang

Pennsylvania State University, University Park, Pennsylvania

WD Burgos, ML Minyard, SL Brantley, DR Hummer, DE Ross, MC Davis, H Tan

Fourier Transform Infrared (FTIR) Characterization of Fe Films Formed on Ephemeral Pool

Portland State University, Portland, Oregon

GH Grathoff, HR Easterly

Whole-Cell and Cytochrome Biological Force Microscopy

Pacific Northwest National Laboratory, Richland, Washington

Cr(VI) Removal from Aqueous Solution Using a Commercial Activated Carbon Coated with Quaternized Poly(4-Vinylpyridine)

Pacific Northwest National Laboratory, Richland, Washington

C Liu

University of Missouri, Columbia, Columbia, Missouri

B Deng

Probing the Structural Network of Buried Water Molecules in the Hydrophobic Core of *Staphylococcal* Nuclease

Johns Hopkins University, Baltimore, Maryland

RL Reynald, EE Lattman

How Redox Proteins on the Exterior of the Outer Membrane of *Shewanella* Accomplish Interfacial Electron Transfer to Fe(III) Oxide Surface

University of Wyoming, Laramie, Wyoming

CM Eggleston

Pacific Northwest National Laboratory, Richland, Washington

TC Droubay

The Surface Structure of *Shewanella* and the Localization of Outer Membrane-Associated Proteins Hypothesized to be Involved in Electron Transfer from Metal-Reducing Bacteria to Metal Oxide Surfaces

University of Guelph, Guelph, Ontario, Canada

TJ Beveridge, JR Dutcher

Pacific Northwest National Laboratory, Richland, Washington

TC Droubay

Mutagenesis and Functional Characterization of *Shewanella oneidensis* Genes Involved in Fe(III) and Mn(IV) Oxide Reduction

Pacific Northwest National Laboratory, Richland, Washington

AS Beliaev, MF Romine, JK Fredrickson

W.R. Wiley Environmental Molecular Sciences Laboratory, Richland, Washington

TW Wietsma

Simulating Mineral Interfaces

University of California, Davis, Davis, California

WH Casey

Pacific Northwest National Laboratory, Richland, Washington

EJ Bylaska

University of California-San Diego, La Jolla, California

JH Weare, SA Bogatko

The Interaction Between Uranium(VI) and Magnetite Surfaces: A Combined Scanning Tunneling Microscopy (STM) and Electron Transfer Calculation Approach

University of Michigan, Ann Arbor, Michigan

FN Skomurski, RC Ewing, U Becker

Strait Science: Biosensor Task 1.1 of the Coastal and Environmental Effects Program

Pacific Northwest National Laboratory, Sequim, Washington

DW Ewert, M Pinza, JR Adamec

Fourier Transform Infrared (FTIR) and Scanning Electron Microscopy (SEM) Characterization of Desert Varnished Rocks

Planetary Science Institute, Pasadena, California

CA Hibbitts

Injection of Zero Valent Iron Evaluation

Pacific Northwest National Laboratory, Richland, Washington

M Oostrom

Laser Fluorescence Analysis of Natural Isotopic Abundance Uranium Oxide Samples

Pacific Northwest National Laboratory, Richland, Washington

JE Amonette

Time-Resolved Laser Spectroscopy of Europium Adsorbed on Gibbsite and Silica

University of Washington, Seattle, Washington

GV Korshin

Determination of Dense, Non-Aqueous-Phase Liquids (DNAPL) Mass Flux Reduction as a Function of Source Zone Mass Removal

University of Arizona, Tucson, Arizona

EL Difilippo, ML Brusseau

Characterization of Novel Arsenic-Iron Precipitates Formed During Biological Iron Reduction

Stanford University, Stanford, California

BD Kocar, S Fendorf, T Borch

Enhancing Carbon Sequestration in Terrestrial Ecosystems: Linking Carbon and Nitrogen Cycling in Soils

Pacific Northwest National Laboratory, Richland, Washington

VL Bailey, SJ Fansler, DW Kennedy

Use of Scanning Electron Microscopy/Transmission Electron Microscopy (SEM/TEM) for Analysis of MR-1 Biofilms Grown for the W.R. Wiley Environmental Molecular Sciences Laboratory (EMSL) Nuclear Magnetic Resonance (NMR) Microscopy

Oregon State University, Corvallis, Oregon

BD Wood

Mineralogical Analysis of Substrates and End-Products of Microbial Fe Redox Transformations

University of Alabama, Tuscaloosa, Tuscaloosa, Alabama

EE Roden

A Theoretical and Experimental Investigation of Multiplet Splitting for Chromium and Uranium Spectra Generated by X-Ray Photoelectron Spectroscopy

University of North Texas, Denton, Texas

PS Bagus

Analysis of Clays Reacted with Simulated Hanford Tank Waste

University of Arizona, Tucson, Arizona

S Choi, JD Chorover

Analysis of Iron Mineralogy of Clay Sediments Exposed to Reducing Conditions

Idaho National Laboratory, Idaho Falls, Idaho

DC Cooper

Microbial Reduction of Iron in Sedimentary Clays: Implications for Subsurface Microbial Ecology and Bioremediation

Miami University, Oxford, Ohio

H Dong

W.R. Wiley Environmental Molecular Sciences Laboratory, Richland, Washington

RK Kukkadapu

Characterization of Biologically Reduced Uranium Particles

Washington State University, Pullman, Washington

BM Peyton, RK Sani

Formulating the CD-MUSIC Surface Complexation Model from First-Principles Calculations for Phosphate Adsorption on Goethite

Virginia Polytechnic Institute, Blacksburg, Virginia

CJ Tadanier

Analyses of Electron Density Distributions in Earth Materials with Implications for Reactivity

Virginia Polytechnic Institute, Blacksburg, Virginia

GV Gibbs

Surface Structure Effects on Direct Reduction of Iron Oxides by *Shewanella oneidensis*

University of Georgia, Aiken, South Carolina

AL Neal

Structure and Reactivity of the Basal and Edge Surfaces of Gibbsite

Brigham Young University, Provo, Utah

BR Bickmore

Critical Point Properties of Electron Density Distributions in High-Pressure Mineral Phases*Virginia Polytechnic Institute, Blacksburg, Virginia*

N Ross

Pressure Effect on Electronic Structure of Anthracene Single Crystals: Formation and Modification of Structural Defects*Washington State University, Pullman, Washington*

ZA Dreger, YM Gupta

Infrared Detection of Organics in Artificial Aging Experiments*Pacific Northwest National Laboratory, Richland, Washington*

CJ Thompson

Gas Chromatography of Solvent-Extracted Organo-Phosphorous Compounds from Soils*Pacific Northwest National Laboratory, Richland, Washington*

J Kelly

W.R. Wiley Environmental Molecular Sciences Laboratory, Richland, Washington

PL Gassman

Investigation into the Polarized Raman Spectra of Benzene, Benzene-d₆, and Hexafluorobenzene*Appalachian State University, Boone, North Carolina*

SD Williams

The Aqueous Thermodynamics and Complexation Reactions of Anionic Silica and Uranium Species to High Concentration*Pacific Northwest National Laboratory, Richland, Washington*

HM Cho, OS Qafoku, Y Xia, Z Wang, ES Ilton

W.R. Wiley Environmental Molecular Sciences Laboratory, Richland, Washington

AR Felmy

Highly Selective Monolayer Sorbents for Advanced Analytical Applications*Pacific Northwest National Laboratory, Richland, Washington*

RS Addleman

U.S. Military Academy, West Point, New York

JT Bays, AE Bjerke

Multi-Resolution Structure and Reactivity of Kinetically Roughened Oxide Surfaces: Nanometric Scaling Behavior and Molecular-Scale Controls*Pacific Northwest National Laboratory, Richland, Washington*

KM Rosso, EJ Bylaska, S Yanina

Idaho National Laboratory, Idaho Falls, Idaho

P Meakin

The Development of Thermodynamic Models for Actinide Species in Mixed Solvent Systems: Application to Binding in Microbial Membranes*Washington State University, Pullman, Washington*

SB Clark

Consortium for Agricultural Soils Mitigation of Greenhouse Gases*Pacific Northwest National Laboratory, Richland, Washington*

JE Amonette

Center for Research on Carbon Sequestration*Pacific Northwest National Laboratory, Richland, Washington*

JE Amonette

Sensor and Tracer Technology for Characterization of Ultra-Low CO₂ Leakage Fluxes*Pacific Northwest National Laboratory, Richland, Washington*

JE Amonette, JL Barr

Model Porous Solids and Sediments*Pacific Northwest National Laboratory, Richland, Washington*

JE Amonette, L Zhong

Biogeochemistry of Uranium Under Reducing and Re-Oxidizing*Pacific Northwest National Laboratory, Richland, Washington*

JE Amonette

Enhancing Carbon Sequestration and Reclamation of Degraded Lands and Sequester Carbon in Soils*Pacific Northwest National Laboratory, Richland, Washington*

JE Amonette

Array-Based Photoacoustic Spectroscopy*Pacific Northwest National Laboratory, Richland, Washington*

JE Amonette, T Autrey, JL Barr

Carbon Tetrachloride Degradation Reaction Mechanisms*Pacific Northwest National Laboratory, Richland, Washington*

JE Amonette, EJ Bylaska

Oregon Health Sciences University/Oregon Graduate Institute, Beaverton, Oregon

PG Tratnyek, V Sarathy

U.S. Environmental Protection Agency (EPA) Consulting: Monitored Natural Attenuation (MNA) of Inorganic Contaminants in Groundwater*Pacific Northwest National Laboratory, Richland, Washington*

JE Amonette

A Bioengineering Approach to the Production of Metal and Metal Oxide Nanoparticles

Temple University, Philadelphia, Pennsylvania

DR Strongin

Chemical Speciation of Americium, Curium, and Selected Tetravalent Actinides in High-Level Waste

Pacific Northwest National Laboratory, Richland, Washington

HM Cho, Z Wang, OS Qafoku, J Boily

Influence of Reactive Transport on the Reduction of U(VI) in the Presence of Fe(III) and Nitrate

Pacific Northwest National Laboratory, Richland, Washington

C Liu, Z Wang

Interactions Between Fe(III): Reducing Bacteria and Fe Oxides—Microbial and Geochemical Dissolution Controls

Pacific Northwest National Laboratory, Richland, Washington

ES Ilton, JM Zachara, KM Rosso

W.R. Wiley Environmental Molecular Sciences Laboratory, Richland, Washington

RK Kukkadapu

Coupling of Fe and Tc Speciation in Subsurface Sediments: Implications to Long-Term Tc Immobilization

Pacific Northwest National Laboratory, Richland, Washington

JM Zachara, A Dohnalkova, BH Lower, J Boily, Z Wang

W.R. Wiley Environmental Molecular Sciences Laboratory, Richland, Washington

RK Kukkadapu

Mineralogic Residence and Desorption Rates of Sorbed ⁹⁰Sr in Contaminated Subsurface Sediments: Implications to Future Beh and In-Ground Stability

Pacific Northwest National Laboratory, Richland, Washington

JM Zachara, C Liu

Characterization of U(VI) Sorption-Desorption Processes and Model Upscaling

Pacific Northwest National Laboratory, Richland, Washington

JM Zachara, C Liu

University of Washington, Seattle, Washington

GV Korshin, H Chang

Science and Technology Road Mapping for Needs from All Sources

Pacific Northwest National Laboratory, Richland, Washington

JM Zachara, Z Wang, M Oostrom

W.R. Wiley Environmental Molecular Sciences Laboratory, Richland, Washington

TW Wietsma

Remediation and Closure Science Project: Subsurface Science Tasks

Pacific Northwest National Laboratory, Richland, Washington

JM Zachara, Z Wang, M Oostrom, NP Qafoku

W.R. Wiley Environmental Molecular Sciences Laboratory, Richland, Washington

TW Wietsma

Influence of Mass Transfer on Bioavailability and Kinetic Rate of U(VI) Biotransformation

Pacific Northwest National Laboratory, Richland, Washington

C Liu, Z Wang, JM Zachara, B Jeon

Reactions and Transport of Toxic Metals in Rock Forming Silicates at 25°C

Pacific Northwest National Laboratory, Richland, Washington

ES Ilton

Actinide Interactions with Environmental Bacteria

Los Alamos National Laboratory, Los Alamos, New Mexico

MP Neu

Characterization of U(VI) Speciation in Samples from Laboratory Batch and Column Experiments

Lawrence Berkeley National Laboratory, Berkeley, California

J Wan, Y Kim

Liquid Infrared Spectroscopy and Spill Phenomenology

Pacific Northwest National Laboratory, Richland, Washington

RS Disselkamp, JL Hylden

W.R. Wiley Environmental Molecular Sciences Laboratory, Richland, Washington

PL Gassman

Movement and Dissolution of a Viscous, Multicomponent Light Nonaqueous-Phase Liquid in a Fluctuating Water Table System

Netherlands Organization for Applied Scientific Research, Utrecht, Netherlands

C Hofstee

Quantification and Chemical Analysis of Iron Oxidation in Microbially Reduced Sediments

W.R. Wiley Environmental Molecular Sciences Laboratory, Richland, Washington

RK Kukkadapu

Princeton University, Princeton, New Jersey

J Komlos, PR Jaffe

Model Development on Using Clay Membranes for Arsenic Removal from Drinking Water

University of Missouri, Columbia, Columbia, Missouri

B Deng

Three-Dimensional Flow and Transport in Highly Heterogeneous Porous Media

Oregon State University, Corvallis, Oregon

BD Wood

Biogeochemical Heterogeneity in the Subsurface

Pacific Northwest National Laboratory, Richland, Washington

T Resch, PE Long

Intermediate Flow Cells

Pacific Northwest National Laboratory, Richland, Washington

T Resch, JE Szecsody

Computational Investigation of Acid Base, Surface Complexation, and Oxidation/Reduction Reaction Mechanisms on Iron Oxide and Silicate Surfaces

University of California, Davis, Davis, California

JR Rustad

Pacific Northwest National Laboratory, Richland, Washington

HM Cho, J Boily

W.R. Wiley Environmental Molecular Sciences Laboratory, Richland, Washington

AR Felmy

The Kinetics of Direct Enzymatic Reduction of Uranium (VI): Effects of Ligand Complexation and U(VI) Speciation

Pacific Northwest National Laboratory, Richland, Washington

CC Ainsworth, KB Wagnon, Z Wang

Enhanced Plutonium Mobility During Long-Term Transport Through an Unsaturated Subsurface Environment: Iron and Manganese Characterization

Westinghouse Savannah River, Aiken, South Carolina

DI Kaplan

Clemson University, Clemson, South Carolina

BA Powell

Uranium Immobilization by Sulfate-Reducing Biofilms

Montana State University, Bozeman, Montana

H Beyenal

Fate of Nitrogen Gas Produced by Denitrification During Uranium and Technetium Bioreduction

Oregon State University, Corvallis, Oregon

JD Istok, MM Park

Interfacial Reduction-Oxidation Mechanisms

Pacific Northwest National Laboratory, Richland, Washington

EC Thornton, JE Amonette

How Aluminum Substitution in Goethite Affects Iron Release

University of California, Berkeley, Berkeley, California

J Cervini-Silva, G Sposito

Characterization of Coupled Hydrologic-Biogeochemical Processes Using Geophysical Data

Pacific Northwest National Laboratory, Richland, Washington

B Arey

Lawrence Berkeley National Laboratory, Berkeley, California

KH Williams

Separation of Corn Fiber and Conversion to Fuels and Chemicals: Pilot Operation

Pacific Northwest National Laboratory, Richland, Washington

DS Muzatko, RJ Orth

Investigation of A Ba-Based NO_x Storage-Reduction Catalyst by Raman Spectrometry

Pacific Northwest National Laboratory, Richland, Washington

D Kim

Influence of Calcium on Aqueous U(VI) Speciation and U(VI) Sorption to the Hanford Sediments

Johns Hopkins University, Baltimore, Maryland

W Ball

Pacific Northwest National Laboratory, Richland, Washington

C Liu

Dissolution and Vaporization of a Mixture of Dense, Non-Aqueous-Phase Liquids (DNAPL) Following a Spill into a Partially Saturated Porous Medium

Auburn University, Auburn, Alabama

JH Dane

U(VI) Speciation and Its Influence on Microbial Reduction in the Presence of Humic Substances

Pacific Northwest National Laboratory, Richland, Washington

C Liu

Oak Ridge National Laboratory, Oak Ridge, Tennessee

B Gu

Photophysics of Organophosphorous Compounds

Pacific Northwest National Laboratory, Richland, Washington

AB Padmaperuma, LS Sapochak

**Influence of Flow on Abiotic and Biotic Reactivity of CL-20
(Hexaanitrohexaazaiso-Wurtzitane)**

Pacific Northwest National Laboratory, Richland, Washington

JE Szecsody, DC Girvin

Conductivity of Bacterial Nanowires

Pacific Northwest National Laboratory, Richland, Washington

YA Gorby, S Yanina, KM Rosso

**Transmission Electron Microscopy Analysis of a Novel Organo-Cr(III) Degrading
Bacterium**

Washington State University, Pullman, Washington

GJ Puzon, L Xun

Mössbauer Spectroscopic Investigations of Fe-Doped SnO₂ Powders

Boise State University, Boise, Idaho

A Punnoose

**Synthesis and Characterization of Limited-Solubility-U(VI)-Bearing Compounds in
Concrete**

Pacific Northwest National Laboratory, Richland, Washington

DM Wellman, S Mattigod

Staff

Nancy S. Foster-Mills, Scientist III, Technical Lead (until September 2005)
(509) 376-1343, nancy.foster@pnl.gov

Nancy J. Hess, Scientist V
(509) 376-3979, nancy.hess@pnl.gov

Kimberly S. Korenkiewicz, Administrator (until September 2005)
(509) 376-1800, kimberly.korenkiewicz@pnl.gov

Paul L. Gassman, Scientist II
(509) 376-7972, pl.gassman@pnl.gov

Ravi Kukkadapu, Scientist IV
(509) 376-3795, ravi.kukkadapu@pnl.gov

Thomas W. Wietsma, Scientist II
(509) 376-6588, wietsma@pnl.gov

We would also like to acknowledge the contributions of James E. Amonette, Eric J. Bylaska, Alice Dohnalkova, Andrew R. Felmy, Eugene S. Ilton, Timothy J. Johnson, Alan G. Joly, Chongxuan Liu, Brian H. Lower, Robert Orr, Martinus Oostrom, Odeta Qafoku, Joy D. Rosscup, Kevin M. Rosso, Colleen K. Russell, Zheming Wang, and John M. Zachara.